Intraband optical absorption in superlattices in an in-plane magnetic field

M. de Dios Leyva*
Instituto di Física, Universidade Estadual de Campinas-Unicamp, Caixa Postal 6165, Campinas, São Paulo 13081-100, Brazil

V. Galindo
Department of Theoretical Physics, University of Havana, San Lazaro y L, Vedado, Ciudad Habana 10400, Cuba
(Received 21 September 1992; revised manuscript received 22 February 1993)

The absorption coefficient of GaAs-$Al_xGa_{1-x}As$ superlattices in an in-plane magnetic field is studied in the case of intraband transitions between electronic magnetic levels. A detailed analysis of the absorption peaks and their dependence on the magnetic-field intensity, superlattice period, and temperature, is performed. By taking into account the detailed properties of the magnetic subbands, the joint density of states, the transition matrix elements, and the effective sheet concentration of electrons involved in the optical transitions, a simple theoretical explanation is given for some experimental results previously reported.

I. INTRODUCTION

The optical properties of superlattices (SL's) under a magnetic field parallel to the layers ($B_{\parallel}$ configuration) have been extensively studied both theoretically and experimentally. Interband magnetoluminescence[1-4] and cyclotron resonance[5-7] have been used to study the magneto-optical properties of SL's in the above-mentioned configuration. Very interesting properties have been established. For example, Belle, Maan, and Weiman[1] and Mann[2-4] have shown, both theoretically and experimentally, that transitions between well-defined Landau levels may be seen in interband magnetoluminescence only for transitions that are related to Landau levels with energies within the first electron and first hole minibands. Most relevant for the present paper are the recent studies on cyclotron resonance in GaAs-$Al_xGa_{1-x}As$ SL's reported by Duffield *et al.*[5,6] and Brozak *et al.*[7] These authors measured the absorption spectra for transitions between magnetic levels within or above the lowest conduction miniband of the SL (electronic magnetic levels). They showed that at low fields, as the cyclotron energy is well within the SL first miniband, the linewidths are relatively sharp, whereas at high fields, as the cyclotron energy approaches the miniband width, the absorption tends to broaden and saturate. Theoretically, Duffield *et al.*[5,6] calculated the absorption spectrum for different values of the magnetic field intensity B, the SL period d, and the temperature T, achieving good agreement with their experimental data. However, in spite of the considerable progress in the understanding of the experimental data,[5-7] up to now we have had no available analysis of the absorption spectra taking into account the detailed properties of the magnetic subbands, the joint density of states, the transition matrix elements, and the effective sheet concentration of electrons which are involved in the optical transitions. Our purpose is to report such an analysis for the case of intraband transitions between electronic magnetic levels.

This work is organized as follows. In Sec. II, the envelope functions, the transition matrix elements, and the joint density of states are presented. In Sec. III, an expression for the absorption coefficient is derived. Results and discussion are presented in Sec. IV. We conclude with a summary in Sec. V.

II. ENVELOPE FUNCTIONS, TRANSITION MATRIX ELEMENTS, AND JOINT DENSITY OF STATES

Our theoretical analysis will be carried out within the envelope-function scheme and in the parabolic-band model, which is a good approximation to study the electronic magnetic levels and the corresponding wave functions in GaAs-$Al_xGa_{1-x}As$ SL's. Plasma-cyclotron resonance will not be considered as justified by Duffield *et al.*[5,6] for the case of low electron concentration and large magnetic fields.

We define z as the growth axis of the SL and consider a magnetic field applied along the y direction. Then, if we choose the gauge $A=(zB,0,0)$, the corresponding envelope functions may be chosen as[8]

$$|\lambda,k_\perp\rangle=\frac{e^{ixk_x}}{(L_x)^{1/2}}\frac{e^{iyk_y}}{(L_y)^{1/2}}\Phi_{\lambda k_x}(z)\ , \tag{1}$$

where $k_\perp=(k_x,k_y)$, $\lambda=0,1,2,\ldots$ indicate the Landau subband index, and L_x and L_y are the linear dimensions of the sample in the x and y directions, respectively. The set of functions in (1), which we assume are orthonormalized, describes states with well-defined values of k_y, the orbit center $z_0=-k_x l_B^2$, and the energy $E_\lambda(k_\perp)=\varepsilon_\lambda(k_x)+\hbar^2k_y^2/2m^*$, where $l_B=(\hbar c/eB)^{1/2}$ is the cyclotron radius, and $\Phi_{\lambda k_x}(z)$ and $\varepsilon_\lambda(k_x)$ are, respectively, the eigenfunctions and eigenvalues of the effective Hamiltonian of Ref. 8 after substituting $\hat{P}_x$ by $\hbar k_x$ and $\hat{P}_y$ by zero. The SL potential $V(z)$ is taken equal to zero inside the wells and V_0 in the barriers. The origin of coordinates (energy) is taken at the center of a well (at the bottom of

the bulk conduction band in the wells). Furthermore, if $d=L_W+L_B$ is the period of the SL, $\varepsilon_\lambda(k_x)$ is an even and periodic function of k_x (of z_0) with period $d/l_B^2(d)$, where L_W and L_B are the thicknesses of well and barrier layers, respectively. In what follows, we assume $|k_x|\leq d/2l_B^2$ ($|z_0|\leq d/2$).

In this work, effects of changes in the effective mass m^* when the electron wave function penetrates the barriers are neglected. The use of this approximation, often employed in the literature, depends on the magnetic-field intensity and on the values taken by the SL parameters. In fact, the effects of taking into account the different values of the effective masses in the wells m_W^* and in the barriers m_B^* may be included in a perturbation which is proportional to a coupling constant $g=(m_B^*-m_W^*)/m_B^*$ and is different from zero only in the barrier layers. In GaAs-$Al_xGa_{1-x}As$ SL's and for low and moderate Al concentrations—where m_B^* and m_W^* are not widely different—these effects may be neglected for narrow barriers ($L_B \ll L_W$ and $L_B \ll l_B$). Under these conditions, which are valid for the most relevant cyclotron-resonance experiments,[5,6] the corrections introduced by using different effective masses in the calculation of magnetic subbands and wave functions should not appreciably modify the results obtained when the constant effective-mass approximation is used. Also, it should be pointed out that the approximation assumed here has been successfully used by Duffield *et al.*[5,6] and Maan and coworkers[1–4] to describe their respective experimental results.

To deal with the experimental situation[5,6] our calculation will be performed in the Voigt geometry. In this case, the polarization vector of the radiation ϵ is parallel to the interfaces and perpendicular to B (ϵ parallel to the x axis). Under these conditions, it is not difficult to show that the matrix element between an initial state $|\lambda,k_\perp\rangle$ and a final state $|\lambda',k_\perp'\rangle$, in the dipole approximation, is given by[8]

$$M_{\lambda'\lambda}(k_\perp',k_\perp)=\delta_{k_\perp',k_\perp}M_{\lambda'\lambda}(k_x)\ , \tag{2}$$

where

$$M_{\lambda'\lambda}(k_x)=\frac{2^{1/2}l_B\hbar\omega_C\langle\Phi_{\lambda'kx}|dV(z)/dz|\Phi_{\lambda kx}\rangle}{[\varepsilon_{\lambda'}(k_x)-\varepsilon_\lambda(k_x)]^2-(\hbar\omega_C)^2} \tag{3}$$

and $\omega_C=eB/cm^*$ is the cyclotron frequency.

The matrix elements (3) are normalized to the matrix element between the ground and first excited Landau levels in the bulk [$V(z)=0$]. From (2), it is obvious that only vertical transitions may occur. Another very useful quantity in the study of the absorption spectra is the joint density of states. For the $\lambda\rightarrow\lambda'$ transition, and neglecting lifetime broadening, this quantity may be defined as

$$J_{\lambda'\lambda}(\varepsilon)=\frac{1}{2\pi d}|d\varepsilon_{\lambda'\lambda}(k_x)/dk_x|^{-1}_{\varepsilon_{\lambda'\lambda}(k_x)=\varepsilon}\ , \tag{4}$$

where $\varepsilon_{\lambda'\lambda}(k_x)=\varepsilon_{\lambda'}(k_x)-\varepsilon_\lambda(k_x)$.

It is straightforward to show that for $\varepsilon=\varepsilon_{\lambda'\lambda}(0)$ and $\varepsilon=\varepsilon_{\lambda'\lambda}(\pm d/2)$, the joint density of states has van Hove–like infinite singularities which are related to the symmetry properties of the system and, in general, are correlated to the resonant structure of the absorption spectra.

III. ABSORPTION COEFFICIENT

The electronic magnetic levels are assumed to be populated in order to study the intraband optical absorption. Experimentally, this condition is satisfied in n-doped semiconductor SL's for sufficiently high temperatures,[5,6] i.e., for $k_BT\gg E_d$, E_d being the binding energy of impurities and k_B the Boltzmann constant. Moreover, low electron concentration (of the order of 10^{15} cm^{-3}) is experimentally required to minimize impurity scattering and to avoid strong plasma-cyclotron resonance coupling.[5,6] In what follows we assume that these conditions are satisfied.

In the dipole approximation, the transition rate (in the Voigt geometry) is given by[9]

$$W(\hbar\omega)=2C^2\frac{\pi}{h}[\hbar/l_B]^2\sum_{\lambda'>\lambda}\sum_{k_\perp k_\perp'}|M_{\lambda'\lambda}(k_\perp',k_\perp)|^2\times[f_\lambda(k_\perp)-f_{\lambda'}(k_\perp')]\times\delta[E_{\lambda'}(k_\perp')-E_\lambda(k_\perp)-\hbar\omega]\ , \tag{5}$$

where C is a constant,[8] $f_\lambda(k_\perp)$ [$f_{\lambda'}(k_\perp')$] is the occupancy of electrons for the state $|\lambda,k_\perp\rangle$ [$|\lambda',k_\perp'\rangle$], and $M_{\lambda'\lambda}(k_\perp',k_\perp)$ are the matrix elements defined in (2). In Eq. (5), the effects associated to scattering of electrons will be considered via a Lorentzian[10] with an energy-broadening parameter Γ_S.

The Fermi energy μ for a given concentration N of electrons is determined using the standard expression

$$N=(2/V)\sum_{\lambda,k_\perp}|f_\lambda(k_\perp)\ , \tag{6}$$

V being the volume of the sample. For low electron concentration and sufficiently high temperatures, which is the case under consideration, the occupancy of electrons $f_\lambda(k_\perp)$ in (5) and (6) may be approximated by the Maxwell-Boltzmann distribution function. One then shows that the absorption coefficient may be written in the form

$$\alpha(\hbar\omega)=\frac{2\pi^2e^2\hbar N}{ncm^*}\gamma_C(\hbar\omega)\times\sum_{\lambda'>\lambda}\int_{-d/2}^{d/2}\frac{dz_0}{d}|M_{\lambda'\lambda}(z_0)|^2n_{\lambda\lambda'}(z_0)\times L[\varepsilon_{\lambda'\lambda}(z_0)-\hbar\omega]\ , \tag{7}$$

where n is the index of refraction, $\gamma_C(\hbar\omega)=\hbar\omega_C/\hbar\omega$,

$$L(\varepsilon_{\lambda'\lambda}-\hbar\omega)=\frac{(\Gamma_S/2\pi)}{(\varepsilon_{\lambda'\lambda}-\hbar\omega)^2+(\Gamma_S/2)^2}\ , \tag{8}$$

$$n_{\lambda\lambda'}(z_0)=\{\exp[-\varepsilon_\lambda(z_0)/k_BT] - \exp[-\varepsilon_{\lambda'}(z_0)/k_BT]\}G^{-1}(T)\ , \quad (9)$$

and

$$G(T)=\sum_{\lambda=0}^{\infty}\int_{-d/2}^{d/2}\frac{dz_0}{d}\exp[-\varepsilon_\lambda(z_0)/k_BT]\ . \quad (10)$$

In Eq. (7), $n_{\lambda\lambda'}(z_0)$ is proportional to the effective sheet concentration of electrons[9] which are involved in the $(\lambda,z_0)\rightarrow(\lambda',z_0)$ transitions. In the next section, the absorption coefficient [see Eq. (7)] will be used to study the properties of the absorption spectrum of SL's in the $B_\parallel$ configuration.

IV. RESULTS AND DISCUSSION

We focus our attention on the GaAs-$Al_xGa_{1-x}As$ SL's considered by Duffield *et al.*[5] and grown by organometallic chemical vapor deposition. For these SL's the period was varied from 10 to 60 nm, whereas the barriers were nominally 2 nm thick with $x\simeq 0.3$, which would correspond to a barrier potential of approximately 0.24 eV. However, according to the fitting procedure of Duffield *et al.*,[5] best agreement with the experimental data of large-period SL's was achieved with a barrier potential of 0.1 eV and 2 nm of thickness, and with $m^*=0.07m_0$, where m_0 is the free-electron mass. As the present work is aimed at explaining and lending physical insight to the experiments by Duffield *et al.*,[5,6] we used, for both short and large periods, the above fitting parameters. We assumed[7] $N=2\times10^{15}/\text{cm}^3$ and $n=3.5$. The energy-broadening parameter Γ_S was taken[5,6] as 3 meV. The envelope functions $\Phi_{\lambda k_x}(z)$ and the magnetic subbands $\varepsilon_\lambda(z_0)$ are obtained by the method of expansion in sine functions recently proposed by Xia and Fan.[11]

In correspondence with the experimental situation,[5,6] we only consider magnetic fields and temperatures for which electrons essentially occupy the lowest magnetic subband. As a result, the main contribution to the absorption coefficient in (7) comes from $0\rightarrow\lambda'$ transitions with $\lambda'\geq 1$. For this reason we only focus our attention on these transitions, and consider three situations.

(1) Cases where $l_B > d/2$ and the lowest magnetic subband is flat.

In Fig. 1, the absorption coefficient is shown for $d=10$ nm, $T=70$ and 170 K, and $B=3$, 10, and 20 T. The corresponding values of l_B are 14.8, 8.1, and 5.7 nm, respectively. One notices that for $B=3$ and 10 T, the absorption spectrum, for a given temperature, exhibits only one absorption peak with intensity increasing when B goes from 3 to 10 T. When $B=20$ T, one observes two absorption features. It is also interesting to note that when T increases from 70 to 170 K, for a given B, the absorption coefficient is reduced.

It will now be suggested that these results can be understood from general considerations and therefore they are valid for every SL when $l_B > d/2$ and the lowest magnetic subband is flat. In fact, for every SL there always exists a certain interval of magnetic fields where

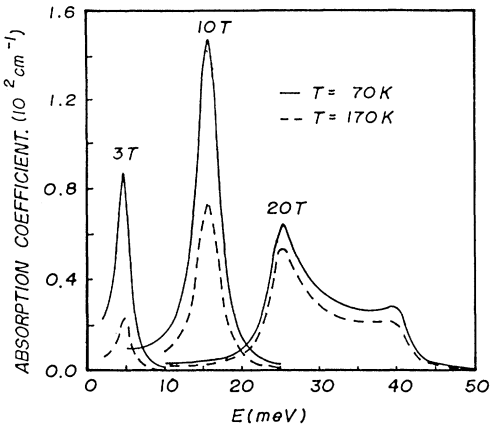

FIG. 1. Absorption coefficient as a function of energy for $d=10$ nm, $T=70$ K (full curves), and 170 K (dashed curves), and $B=3$, 10, and 20 T.

$l_B \gg d/2$ and the $\lambda=0,1$ magnetic subbands are flat,[4] i.e., $\varepsilon_0(z_0)$, $\varepsilon_1(z_0)$, and $\varepsilon_{10}(z_0)$ are practically independent of z_0. This regime was investigated by Duffield *et al.*,[12] who showed that the results of cyclotron resonance can be described in the effective miniband mass approximation (miniband regime). Here, ε_{10} is an increasing and almost linear[4] function of B and therefore the ratio $\hbar\omega_C/\varepsilon_{10}$ is practically B independent. The above considered SL with $d=10$ nm and $B=3$ and 10 T satisfies these conditions [see Figs. 1(a) and 2(a) in Ref. 8]. In the miniband regime, the following considerations are valid:

(a) The transition strength $T_{10}(z_0)=|M_{10}(z_0)|^2$ is approximately equal to 1 and independent of z_0 and B, whereas the $0\rightarrow\lambda'$ transition strengths $T_{\lambda'0}(z_0)=|M_{\lambda'0}(z_0)|^2$, with $\lambda'\geq 2$, are very small[8] (more than four orders of magnitude smaller than T_{10}). According to Eq. (7) and the physical conditions under which the experiments are performed ($N\simeq 10^{15}$ cm^{-3} and $\Gamma_S\simeq 1-3$ meV), the absorption coefficient is, in general, of the order of, or smaller than, 10^2 cm^{-1}. The above results allow us to conclude that in the miniband regime each absorption spectrum will only exhibit one peak, which is associated with the $0\rightarrow 1$ transition and ε_{10} is essentially the cyclotron-resonance energy. Notice that when B increases, neither T_{10} nor the factor $\gamma_C(\hbar\omega)$ in (7) affect the corresponding peak intensity. This is due to the fact that T_{10} and $\gamma_C(\hbar\omega)$, when evaluated at the resonance energy $\hbar\omega_R\simeq\varepsilon_{10}$, are B independent.

(b) As ε_{10} increases with B, when B increases, for a given temperature, the electronic population in the $\lambda=0$ level also increases, whereas it decreases is the higher levels. Therefore, as $T_{10}(z_0)$ and $\gamma_C(\varepsilon_{10})$ in (7) are practically B independent, if B increases the corresponding absorption peak becomes more intense. This effect is illustrated in Fig. 1 when B changes from 3 to 10 T.

Qualitatively, the results of the preceding analysis provide a simple explanation for some of the experimental results reported by Duffield *et al.*[6] (see Fig. 3 in Ref. 6).

Let us now consider those magnetic fields for which $l_B > d/2$, the $\lambda=0$ level is flat, and the $\lambda=1$ level is dispersive. In this case, illustrated in Fig. 2 for $d=10$ nm and $B=20$ T, we are in the miniband breakdown regime as discussed by Duffield *et al.*[6] In general, this case is characterized by the fact that $\varepsilon_{10}(z_0)$ presents only two extrema—one maximum and one minimum at $z_0=0$ and $|z_0|=d/2$, respectively. At these values of $\varepsilon_{10}(z_0)$, the joint density of states $J_{10}(\varepsilon)$ in Eq. (4) exhibits van Hove–like singularities and therefore the absorption spectrum should exhibit at least two structures with resonance energies approximately equal to $\varepsilon_{10}(\pm d/2)$ and $\varepsilon_{10}(0)$, respectively. These two features are associated with the $0\rightarrow 1$ transition and, as discussed by Duffield *et al.*,[5,6] they may be ascribed to tunneling or barrier-bound resonance in which the electron tunnels twice per cycle through a SL barrier and well-bound resonance, respectively. A necessary condition for their experimental observation is determined by the inequality $\varepsilon_{10}(0)-\varepsilon_{10}(\pm d/2)>\Gamma_S$. This result is illustrated in Fig. 1 for $B=20$ T. Furthermore, in this case the possibility of observing more structures—for $\lambda'\geq 2$—is very limited. This is due to the fact that for $l_B > d/2$ the $0\rightarrow\lambda'$ transition strengths, with $\lambda'\geq 2$, are very small. For instance, for $d=10$ nm and $B=20$ T, the transition strengths $T_{\lambda' 0}(z_0)$ with $\lambda'\geq 2$ are of the order of or less than 10^{-2}. We shall return to this point later, when considering the cases where $l_B < d/2$.

In what follows, an important property of the $T_{10}(z_0)$ transition strength which will be often used is related to the following sum rule, which is straightforward to demonstrate:

$$\sum_{\lambda'=0}^{\infty}\{[\varepsilon_{\lambda'}(z_0)-\varepsilon_{\lambda}(z_0)]/\hbar\omega_C\}T_{\lambda'\lambda}(z_0)=1 \ .$$

Calculations performed[8] for the $0\rightarrow\lambda'$ transitions indicate that, for every z_0, the leading term in Eq. (11) is the one associated with the $0\rightarrow 1$ transition. Therefore, one obtains $T_{10}(z_0)\simeq\hbar\omega_C/[\varepsilon_1(z_0)-\varepsilon_0(z_0)]$ and the largest (smallest) values of the transition strength $T_{10}(z_0)$ are reached for values of z_0 close to those for which the $\lambda=0,1$ magnetic subbands are nearest to (farther apart from) each other.

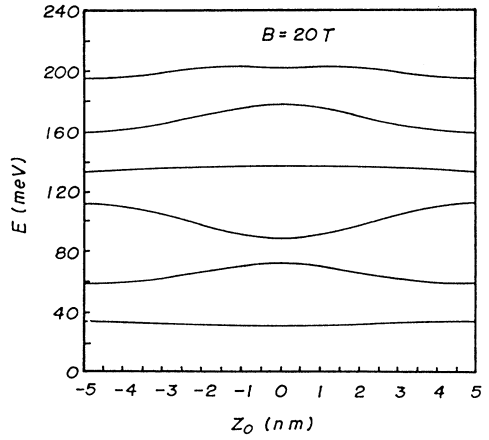

FIG. 2. Magnetic energy levels as a function of the orbit center position for $d=10$ nm and $B=20$ T.

It is also important to note the following. If $\hbar\omega_R$ is any of the resonance energies, therefore, due to the presence of the Lorentzian function in Eq. (7), the main contribution to the corresponding peak height comes from orbits centered in the region where $|\varepsilon_{10}(z_0)-\hbar\omega_R|\lesssim\Gamma_S$.

Bearing the above results in mind, let us now study some other properties of the absorption spectra which characterize the breakdown regime: in this case, $\varepsilon_{10}(0)>\varepsilon_{10}(\pm d/2)$, and the inequalities $\gamma_C[\varepsilon_{10}(\pm d/2)]>\gamma_C[\varepsilon_{10}(0)]$ and $T_{10}(\pm d/2)>T_{10}(0)$ are satisfied. If the breakdown regime is reached for sufficient high magnetic fields, i.e., for $k_BT<\varepsilon_{10}(\pm d/2)$, then $n_{10}(0)\simeq n_{10}(\pm d/2)$, and the absorption peak associated to $\hbar\omega_R\simeq\varepsilon_{10}(\pm d/2)$ (barrier-bound resonance) is more intense than the structure at $\hbar\omega_R\simeq\varepsilon_{10}(0)$ (well-bound resonance). This is illustrated in Fig. 1 for $B=20$ T. For this particular case, $\gamma_C[\varepsilon_{10}(0)]\simeq 0.8$, $\gamma_C[\varepsilon_{10}(\pm d/2)]\simeq 1.32$, $T_{10}(0)\simeq 0.8$, and $T_{10}(\pm d/2)\simeq 1.3$. From the preceding analysis, it is clear that in the breakdown regime the barrier-bound resonances dominate the absorption spectra. This same conclusion was established by Duffield *et al.*[6] through the analysis of their experiments. Our analysis provides a simple explanation of this important property.

In the miniband regime $\varepsilon_{10}(z_0)$ is practically flat and all possible orbits ($|z_0|\leq d/2$) contribute to the peak intensity, whereas in the breakdown regime $\varepsilon_{10}(z_0)$ is dispersive and therefore only those orbits centered in the regions in which $|\varepsilon_{10}(z_0)-\varepsilon_{10}(\pm d/2)|\lesssim\Gamma_S$ and $|\varepsilon_{10}(z_0)-\varepsilon_{10}(0)|\lesssim\Gamma_s$ effectively contribute to the intensity of the peaks associated with barrier-bound and well-bound resonances, respectively. Another important fact in (7) is that the factors $\gamma_C[\varepsilon_{10}(z_0)]$, $T_{10}(z_0)$, and $n_{01}(z_0)$, when evaluated at $z_0=\pm d/2$ and $z_0=0$, are in general slowly varying functions of B (for fixed values of d and T). It then follows that when B increases and the absorption spectrum continuously evolves from the miniband regime to the breakdown regime, the two peaks of the latter case are less intense than the peak of the former. In particular, this conclusion is illustrated in Fig. 1 when B changes from 10 to 20 T. On the other hand, as the $\lambda=0$ subband is always flat, when T increases for d and B given, the electronic population in the higher levels also increases with a decrease of population in the $\lambda=0$ subband. Therefore, as T increases the absorption coefficient is reduced as shown in Fig. 1.

(2) Cases where l_B is of the order of $d/2$ and the two lowest magnetic subbands are dispersive.

Let us now consider those magnetic fields for which the two lowest subbands are dispersive and l_B is of the order of $d/2$. In this case we are again in the breakdown regime. In order to illustrate this situation, in Fig. 3 the absorption coefficient is shown for $d=20$ nm, $T=70$ and 170 K, and $B=7$ and 10 T. For these values of B, $l_B=9.7$ and 8.1 nm, respectively. For this particular case, the most interesting properties of the absorption

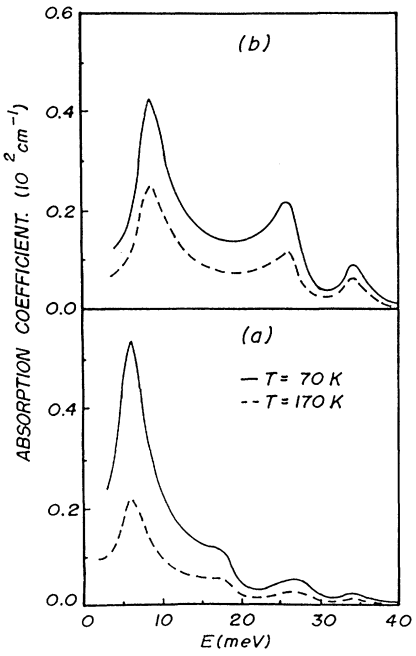

FIG. 3. Absorption coefficient as a function of energy for $d=20$ nm, $T=70$ K (full curves), and 170 K (dashed curves), and (a) $B=7$ T and (b) $B=10$ T.

spectrum for a given temperature are the following: for $B=7$ T, the absorption curve exhibits a sharp peak, whose intensity decreases when B changes from 7 to 10 T, and three structures with less intensity. Two of these features have increasing intensities as B increases from 7 to 10 T, whereas the third one tends to disappear. If T increases for a given B, the absorption coefficient and the peak intensities are reduced.

The magnetic subbands associated with $B=7$ and 10 T and $d=20$ nm are shown in Fig. 4. One can see that $\varepsilon_1(z_0)$ and $\varepsilon_{10}(z_0)$ have only two extrema: one maximum at $z_0=0$ and one minimum at $|z_0|=d/2$. Similarly, $\varepsilon_0(z_0)$ has a minimum at $z_0=0$ and a maximum at $|z_0|=d/2$. In what follows we suppose that these properties are valid for every SL when l_B is of the order of $d/2$ and the two lowest levels are dispersive. All the analyses and calculations carried out with different SL's corroborate this supposition. It is then obvious that two of these absorption peaks (the two peaks associated with the lowest resonance energies in Fig. 3) are associated with the $0\rightarrow 1$ transition and the corresponding resonance energies are approximately given by $\varepsilon_{10}(\pm d/2)$ (barrier-bound resonance) and $\varepsilon_{10}(0)$ (well-bound resonance), respectively. As $\varepsilon_{10}(\pm d/2)<\varepsilon_{10}(0)$, it is obvious that $\gamma_C[\varepsilon_{10}(0)]<\gamma_c[\varepsilon_{10}(\pm d/2)]$ and $T_{10}(0)<T_{10}(\pm d/2)$. It is then apparent from Eq. (7) that the absorption peak associated with $\hbar\omega_R\simeq\varepsilon_{10}(\pm d/2)$ is favored by these inequalities. However, as $\varepsilon_0(0)<\varepsilon_0(\pm d/2)$ and $\varepsilon_1(0)>\varepsilon_1(\pm d/2)$, we have $n_{01}(0)>n_{01}(\pm d/2)$. As a result, the peak at $\hbar\omega_R\simeq\varepsilon_{10}(0)$ is favored by this inhomogeneous distribution of electrons. Therefore, if this inhomogeneity is not very important, the peak localized at $\hbar\omega_R\simeq\varepsilon_{10}(\pm d/2)$ will be more intense than the peak at $\hbar\omega_R\simeq\varepsilon_{10}(0)$. In this case, barrier-bound resonances dominate the absorption spectra, which is again in perfect agreement with the cyclotron-resonance experiments reported by Duffield *et al.*[6] This situation is illustrated in Fig. 3(a), where in correspondence with Fig. 4(a), $\varepsilon_{10}(\pm d/2)$ and $\varepsilon_{10}(0)$ are approximately the resonance energies of the sharp peak and of the weak feature nearest to it, respectively. However, as B increases, the effects associated to the abovementioned inhomogeneity become more and more important and therefore the well-bound resonance develops at the expense of the barrier-bound resonance. This evolution is illustrated in Fig. 3 when B changes from 7 to 10 T. If the magnetic field is further increased, it is apparent that there exists a range of values of magnetic-field intensities for which the barrier-bound resonance and the well-bound resonance are equally important.

With respect to the weak feature associated with $\hbar\omega_R\simeq 34.5$ meV in Fig. 3(a), a comparison between this energy and the magnetic subbands shown in Fig. 4(a) indicates that $|\varepsilon_{30}(z_0)-34.5\text{ meV}|\lesssim\Gamma_S$ for every $|z_0|\lesssim 4$

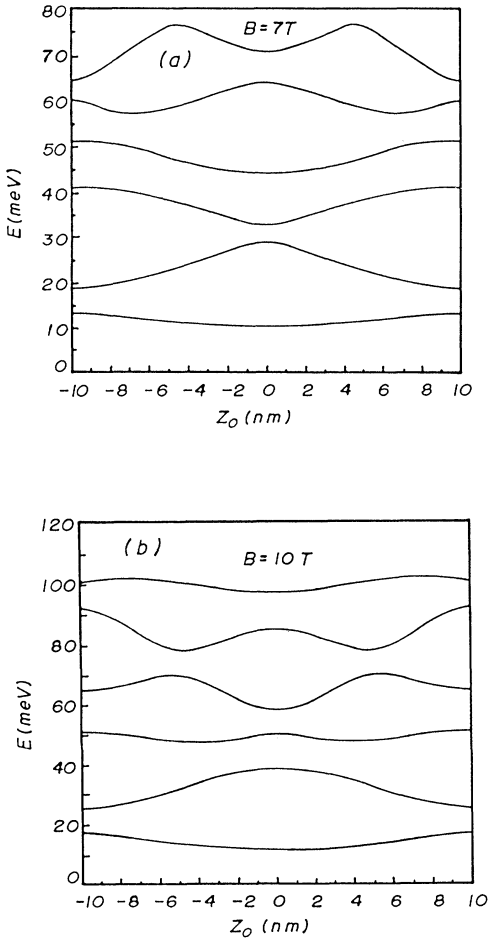

FIG. 4. Magnetic energy levels as a function of the orbit center position for $d=20$ nm and (a) $B=7$ T and (b) $B=10$ T.

nm. Notice that $\varepsilon_{30}(z_0)$ is a very slow function of z_0 in this interval. Moreover, the joint density of states $J_{30}(\varepsilon)$ exhibits a van Hove–like singularity at $\varepsilon=\varepsilon_{30}(0)$ and, for $z_0\simeq 0$, the $0\rightarrow 3$ transition strength is *not* very small $[T_{30}(0)\simeq 0.1]$ and, therefore, the structure at $\hbar\omega_R\simeq 34.5$ meV appears as a weak feature in the absorption spectrum. However, not all orbits centered in the interval $|z_0|\lesssim 4$ nm effectively contribute to its intensity. In fact, $T_{30}(z_0)$ shows a strong dependence on z_0, taking its maximum value at $z_0=0$ $[T_{30}(0)\simeq 0.1]$ and rapidly decreasing as $|z_0|$ increases. For instance, $T_{30}(z_0)\simeq 10^{-2}$ for $|z_0|=4$ nm. So, the weak feature at $\hbar\omega_R\simeq 34.5$ meV may be ascribed to a $0\rightarrow 3$ well-bound resonance centered on the neighborhood of $z_0=0$. For $d=20$ nm and $B=10$ T, the z_0 dependence of $T_{30}(z_0)$ is very similar to that of the preceding case ($d=20$ nm and $B=7$ T), except that $T_{30}(0)$ is an order of magnitude smaller as B increases from 7 to 10 T, and therefore the corresponding feature tends to disappear when B is increased.

Let us now consider the feature with resonance energy $\hbar\omega_R\simeq 27$ meV in Fig. 3(a). First, one should notice that $\varepsilon_{20}(z_0)$ is a slowly varying function of z_0 [cf. Fig. 4(a)]. Also, according to Figs. 3(a) and 4(a), $|\varepsilon_{20}(z_0)-27$ meV $|\lesssim\Gamma_S$ for every z_0 in the interval 2 nm $\lesssim|z_0|\lesssim 10$ nm. In this case, the transition strength $T_{20}(z_0)$ shows a strong dependence on z_0, with maximum value at $|z_0|\simeq 5$ nm $[T_{20}(|z_0|\simeq 5\text{ nm})\simeq 0.2]$ and decreasing to zero as $|z_0|$ tends to 10 nm or to zero, respectively. In fact, the main contribution to the peak intensity for $B=7$ T comes from orbits centered on the interval 3 nm $\lesssim|z_0|\lesssim 7$ nm. When B increases to 10 T, the main contribution to the peak intensity then comes from orbits centered on the interval 4 nm $\lesssim|z_0|\lesssim 8$ nm [see Figs. 3(b) and 4(b)]. In this interval, $0.1\lesssim T_{20}(z)\lesssim 0.2$, and $\varepsilon_{20}(z_0)$ becomes essentially flat [see Fig. 4(b)] which explains why the peak intensity in Fig. 3 increases when the magnetic field is changed from 7 to 10 T.

(3) Cases where $l_B\ll d/2$.

Actually, in this section we are interested in the study of the absorption spectra when $l_B\ll L_W/2$. This is an interesting limiting case for which there exist intervals of z_0 for which the corresponding classical electron orbits shrink inside the well.[2]

In Fig. 5 the absorption coefficient as a function of energy is shown for $L_W=48$ nm ($d=50$ nm), $T=70$ and 170 K, and $B=7$ and 10 T. For these values of B, $l_B=9.7$ and 8.1 nm, respectively, which are much smaller than $L_W/2$. One can see that the absorption spectra exhibit a sharp peak situated between two small shoulders and the resonance may be characterized as an extremely inhomogeneously broadened line.[5] As B increases, going from 7 to 10 T, the intensity of the sharp peak is enhanced. Moreover, when T increases for a given B, the absorption coefficient is reduced.

In general, for $l_B\ll d/2$, the most important characteristics of the energy spectrum are illustrated in Fig. 6 in the case of $d=50$ nm and $B=10$ T, and may be understood as follows: each magnetic subband λ is strongly dispersive only for those values of z_0 at a distance less than $(2\lambda+1)^{1/2}l_B$ from each interface, whereas it is almost flat outside such an interval. This property corresponds to the intuitive classical image that the energy levels will only change when the cyclotron orbit touches each barrier.[4] Therefore, from a magneto-optical point of view, the most important properties of the magnetic levels are essentially displayed in Fig. 6.

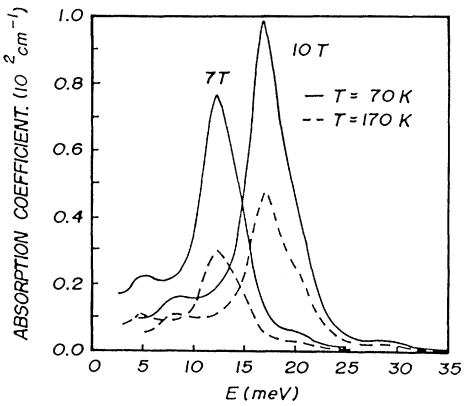

FIG. 5. Absorption coefficient as a function of energy for $d=50$ nm, $T=70$ K (full curves) and 170 K (dashed curves), and $B=7$ and 10 T.

In Fig. 5, the shoulder of the lowest resonance energy $[\hbar\omega_R\simeq\varepsilon_{10}(\pm d/2)]$ and the sharp peak $[\hbar\omega_R\simeq\varepsilon_{10}(0)]$ are associated with the $0\rightarrow 1$ transition and the main contribution to the corresponding peak intensities comes from orbits centered on the neighborhood of $|z_0|=d/2$ (barrier-bound transitions) and $z_0=0$ (well-bound transitions), respectively. It follows from Fig. 6 that $\varepsilon_{10}(\pm d/2)<\varepsilon_{10}(0)$, $\varepsilon_0(0)<\varepsilon_0(\pm d/2)$, and $\varepsilon_1(0)>\varepsilon_1(\pm d/2)$. Therefore, for $|z_0|=d/2$ and $z_0=0$, the factors $\gamma_C(\hbar\omega)$, $T_{10}(z_0)$, and $n_{01}(z_0)$ satisfy the same inequalities as in the cases discussed above (when l_B is of the order of $d/2$ and the two lowest magnetic levels are dispersive). However, for $l_B\ll d/2$, the effects associated with the inhomogeneous distribution of electrons $[n_{01}(0)>n_{01}(\pm d/2)]$ are more important and, therefore, the well-bound transitions tend to dominate the spectra. Another very important effect which favors these last

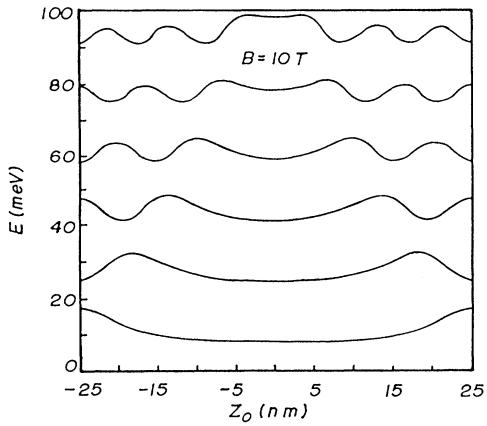

FIG. 6. Magnetic energy levels as a function of the orbit center position for $d=50$ nm and $B=10$ T.

transitions is associated to the fact that $\varepsilon_{10}(z_0)$ is practically flat in the interval $|z_0| \lesssim L_W/2 - l_B$ and, therefore, all orbits centered on it effectively contribute to the corresponding peak intensity. The preceding effects explain why in the extreme limit of large magnetic field ($l_B \ll d/2$) well-bound resonances dominate the absorption spectra. This result is also in agreement with the studies by Duffield *et al.*[5,6] Furthermore, when B increases, for given d and T, both the interval $|z_0| \lesssim L_W/2 - l_B$ and the difference $n_{01}(0) - n_{01}(\pm d/2)$ also increase. It is then clear that the intensity of the peak associated with the well-bound resonance increases with the magnetic field. This effect, illustrated in Fig. 6 (sharp peak) when B increases from 7 to 10 T, has been observed in cyclotron-resonance experiments.[13]

Let us now briefly consider the $B=10$ T small shoulder with resonance energy $\hbar\omega_R \simeq 28$ meV (cf. Fig. 5). For $B=7$ T, the magnetic subbands and the transition strengths are completely similar to the 10-T case and therefore here we will only discuss the 10-T shoulder which is obviously the evolution of the peak with highest resonance energy in Fig. 3(b). Now, a comparison between its resonance energy, $\hbar\omega_R \simeq 28$ meV, and the magnetic subbands illustrated in Fig. 6 indicates that $|\varepsilon_{20}(z_0) - 28 \text{ meV}| \lesssim \Gamma_S$ for every z_0 in the interval 17 nm $\lesssim |z_0| \lesssim$ 25 nm. Actually, this interval should be reduced on its right side because the $0 \rightarrow 2$ transition is forbidden by symmetry at the barrier center, i.e., $|z_0| = 25$ nm. Then, the main contribution to the peak intensity comes from orbits centered in the reduced interval. Notice that the occurrence of this small shoulder is associated with the fact that $\varepsilon_{20}(z_0)$ has a minimum at $|z_0| \simeq 19$ nm and therefore the joint density of states exhibits a van Hove–like singularity at $\varepsilon \simeq \varepsilon_{20}$ (± 19 nm). The intensity of this small shoulder is reduced when l_B decreases (B increases) because then the $0 \rightarrow 2$ transition strength tends to be very small for every z_0.

Finally, when the magnetic levels are dispersive the lowest Landau levels in the $\lambda=0$ subband are localized in the neighborhood of $z_0=0$. As a result, for a given d and B, when T increases, $n_{01}(0)$ must always decrease and therefore the intensity of the peak associated with the well-bound resonances is reduced (see Figs. 3 and 5). This thermal effect was observed and discussed by Duffield *et al.* in Ref. 5. Due to the inequality $\varepsilon_0(\pm d/2) > \varepsilon_0(0)$, the situation is different for barrier-bound resonances. In fact, as T increases, the effective electronic population for the barrier-bound states and involved in the $0 \rightarrow 1$ transition varies according to the following mechanisms: it decreases due to thermal excitation toward barrier-bound states in the $\lambda=1$ magnetic subband and it increases due to thermal excitation from the lowest magnetic levels in the $\lambda=0$ subband to barrier-bound states in the same subband. The behavior of the peak intensity associated with the barrier-bound resonances will depend on which mechanism is the dominant one. If the first (second) mechanism dominates, the corresponding peak intensity is reduced (enhanced) as shown in Fig. 5. An experimental situation where the barrier-bound resonance is enhanced (when the temperature was increased) may be found in Ref. 5.

V. SUMMARY

We have studied the absorption spectra associated with transitions ($0 \rightarrow \lambda'$, with $\lambda' \geq 1$) between electronic magnetic levels for GaAs-$Al_xGa_{1-x}As$ SL's in the $B_{\parallel}$ configuration. The number of peaks in each absorption curve, their properties and evolution, depend on the range of considered magnetic fields. For a given temperature we have shown that the absorption spectrum exhibits only one peak in the miniband regime and two peaks in the breakdown regime (when the lowest magnetic subband is flat). In both cases these peaks are associated with the $0 \rightarrow 1$ transition and in the breakdown regime the spectra are dominated by barrier-bound resonances. In the breakdown regime, when the two lowest magnetic subbands are dispersive, the spectra may exhibit more than two peaks, but the most prominent peaks are associated with the $0 \rightarrow 1$ transition. In this case, there exists a range of intensities of the magnetic field for which the absorption spectra are dominated by barrier-bound resonance and another for which barrier-bound and well-bound resonances are equally important. In the extreme limit of large magnetic fields the spectra are inhomogeneously broadened to high and low energies and are dominated by well-bound resonances. To our knowledge, only the $0 \rightarrow 1$ absorption peaks have been seen experimentally.[5,7,12,13] This is due to the fact that the heights of the remaining peaks ($0 \rightarrow \lambda'$, with $\lambda' \geq 2$) are relatively small and therefore its observation would be very difficult.

Summing up, we believe the results of our analysis provide a simple explanation for most of the observations previously reported and clarify and lend physical insight to them.

M.D.L. would like to acknowledge the Brazilian Conselho Nacional de Desenvolvimento Cientifico e Tecnológico CNPq for financial support while at subbatical leave at the Universidade Estadual de Campinas, and the International Energy Agency and UNESCO for hospitality at the International Centre for Theoretical Physics, Trieste, where part of this work was done.

*Permanent address: Dept. of Theoretical Physics, University of Havana, San Lazaro y L, Vedado, Ciudad Habana, 10400, Cuba.

[1]G. Belle, J. C. Maan, and G. Weimann, Solid State Commun. **56**, 65 (1986); Surf. Sci. **170**, 611 (1986).

[2]J. C. Maan, in *Two-Dimensional Systems, Heterostructures and Superlattices*, edited by G. Bauer, F. Kuchar, and H. Heinrich Springer Series in Solid State Sciences Vol. 53 (Springer, Berlin, 1984), p. 183.

[3]J. C. Maan, Surf. Sci. **196**, 518 (1988).

[4]J. C. Maan, Festkoerperprobleme **27**, 137 (1987).

[5]T. Duffield, R. Bhat, M. Koza, F. DeRosa, K. M. Rush, and S.

J. Allen, Jr., Phys. Rev. Lett. **59**, 2693 (1987).
[6]T. Duffield, R. Bhat, M. Koza, D. M. Hwang, F. DeRosa, P. Grabbe, and S. J. Allen, Jr., Solid State Commun. **65**, 1483 (1988).
[7]G. Brozak, E. A. de Andrade e Silva, L. J. Sham, F. DeRosa, P. Miceli, S. A. Schwarz, J. P. Harbison, L. T. Florez, and S. J. Allen, Jr., Phys. Rev. Lett. **64**, 471 (1990).
[8]M. de Dios-Leyva, V. Galindo, and J. Lopez-Gondar, Phys. Rev. B **45**, 1923 (1992).
[9]S. Nojima, Phys. Rev. B **41**, 10 214 (1990).
[10]J. J. Sakurai, *Modern Quantum Mechanics* (Benjamin/Cummings, Menlo Park, CA, 1985), Sec. 5.7.
[11]J. B. Xia and W. J. Fan, Phys. Rev. B **40**, 8508 (1989).
[12]T. Duffield, R. Bhat, M. Koza, F. DeRosa, D. M. Hwang, P. Grabbe, and S. J. Allen, Jr., Phys. Rev. Lett. **56**, 2724 (1986).
[13]S. J. Allen, Jr., T. Duffield, R. Bhat, M. Koza, M. C. Tamargo, J. P. Harbison, F. DeRosa, D. M. Hwang, P. Grabbe, and K. M. Rush, in *Proceedings of the International Conference on High Magnetic Field in Semiconductor Physics,* edited by G. Landwehr, Springer Series in Solid State Sciences Vol. 71 (Springer, Berlin, 1987), p. 184.